Supporting Information

Towards a wearable format for transducing responsive swelling in hydrogels using impedance

Rinki Singh[*1], Dinakaran Thirumalai[1], Tanya Levingstone[2] and Aoife Morrin[*1]

[1]School of Chemical Sciences, Insight Research Ireland for Data Analytics, Dublin City University, D09 V209, Ireland

[2]School of Mechanical Engineering, Dublin City University, D09 V209, Ireland

E-mail: aoife.morrin@dcu.ie; rinkoosingh62@gmail.com

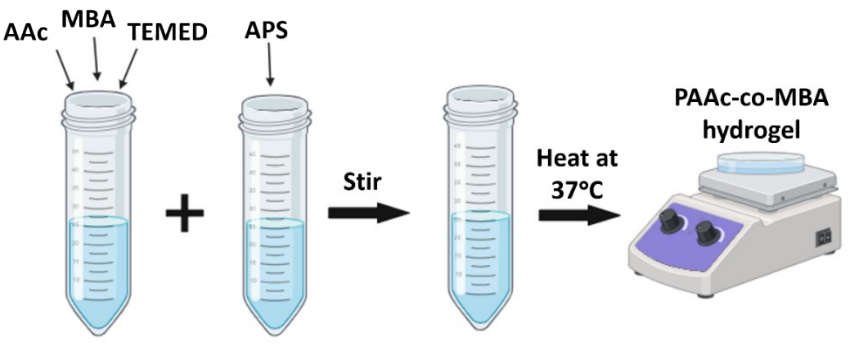

Figure S1. Schematic of PAAc-co-MBA hydrogel synthesis method using a free radical polymerisation reaction (as described in Methods Section 2.2).

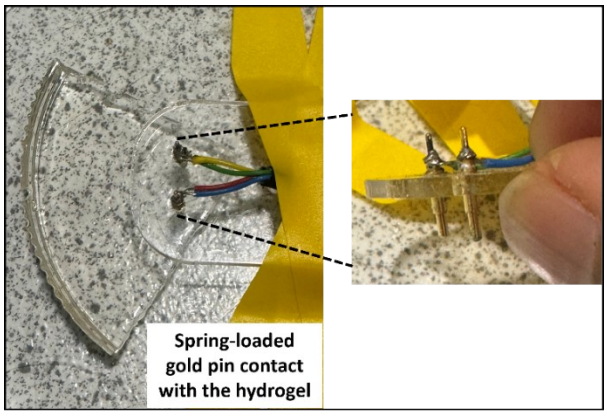

Figure S2. Electrode setup for EIS measurements of hydrogel swelling (as described in Methods Section 2.3).

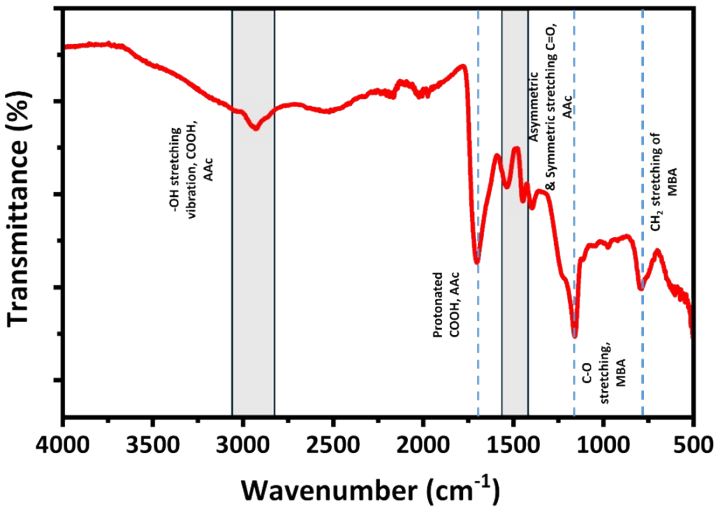

Figure S3. ATR-FTIR spectra. PAAc-co-MBA hydrogel composition used: 20% AAc, 1.5% MBA, 8.8% APS. It confirms the formation of the hydrogel as shown in Scheme 1. The broad absorption band observed at 2959 cm^{-1} is assigned to the –OH stretching vibration of carboxylic acid groups originating from acrylic acid[1, 2]. The characteristic absorption band at 1705 cm^{-1} corresponds to the C=O stretching vibration of protonated carboxyl (–COOH) groups, confirming the presence of PAAc within the copolymer network[3-5]. The bands observed at 1537 cm^{-1} and 1455 cm^{-1} are attributed to the asymmetric and symmetric stretching vibrations of carboxylate ($–COO^-$) groups, respectively[3, 6]. In addition, the strong band at 1163 cm^{-1} is assigned to the C–O stretching vibration of the ester group in the MBA crosslinker, while the peak at 789 cm^{-1} corresponds to the $–CH_2$ vibrations of the MBA methyl ester group[4, 7, 8]. Furthermore, the band observed at 1448 cm^{-1}, attributed to C–N stretching, provides further evidence of the successful incorporation and crosslinking of MBA within the PAAc network[9, 10]. Collectively, these characteristic absorption features confirm the successful formation of the PAAc-co-MBA hydrogel structure.

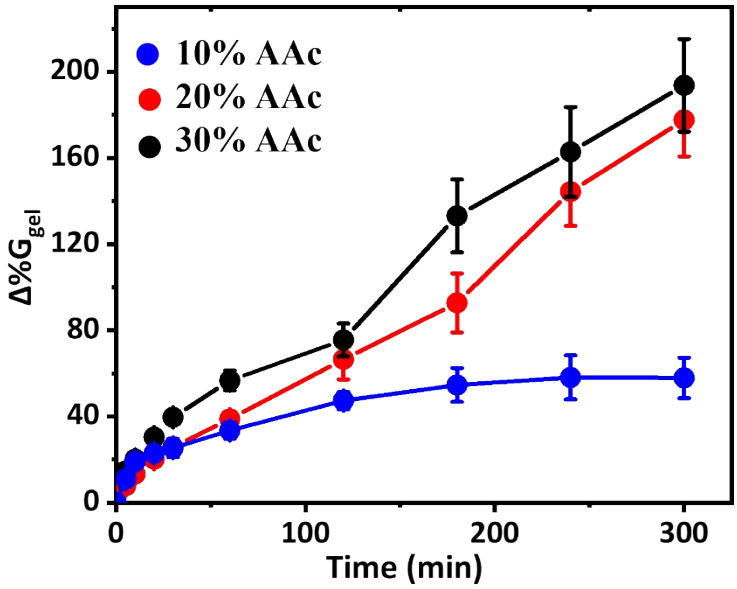

Figure S4. $\Delta\%G_{gel}$ over swelling time for hydrogel quadrants (n=3). PAAc-co-MBA hydrogel composition: 10%, 20% and 30% AAc, 1.5% MBA, 8.8% APS.

Table S1. $\Delta\%R_{gel}$ and $\Delta\%G_{gel}$ values of PAAc-co-MBA hydrogels (20% AAc, 1.5% MBA, 8.8% APS) immersed in 100 mL of DI water over a swelling time of 300 min.

AAc, % v/v	$\Delta\%R_{gel}$	$\Delta\%G_{gel}$
20	658	177

Table S2. Electrical component values of the proposed circuit are fitted to the measured impedance spectrum data of Equation 3. PAAc-co-MBA hydrogel composition: 20% AAc, 1.5% MBA, 8.8% APS (see Figure 1).

Parameters	Parameter values	Error, %
R_{gel}	124.72 Ω	1.7112
$R_{ele\text{-}inter}$	2585.8 Ω	1.8945
CPE1	7.7931E-05	2.897
CPE2	3.1484E-06	2.3106

Table S3. $\Delta\%R_{gel}$ and $\Delta\%G_{gel}$ of PAAc-co-MBA hydrogels (20%AAc) with varying concentrations of MBA and APS for the 300 min swelling time.

Parameter	MBA (8.8% APS)			APS (0.15% MBA)		
	1.5%	0.75%	0.15%	8.8%	2.3%	1.5%
$\Delta\%R_{gel}$	658	862	1115	1115	606	567
$\Delta\%G_{gel}$	177	465	1277	1277	1856	1503

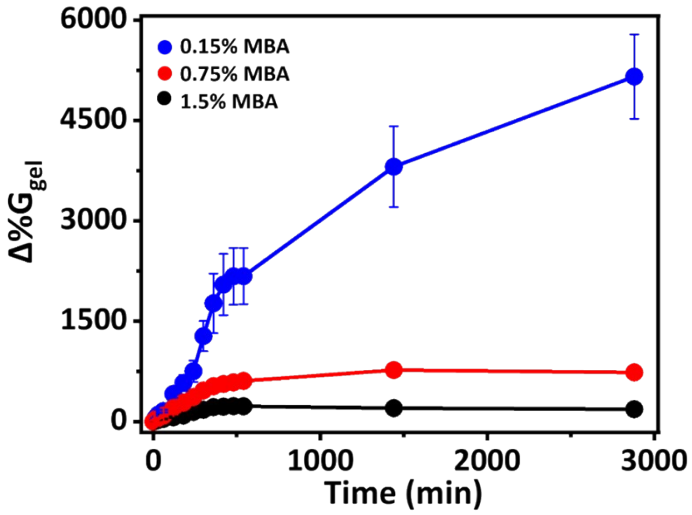

Figure S5. $\Delta\%G_{gel}$ for hydrogel quadrants over time with varying MBA concentrations, n=3 for all measurements. PAAc-co-MBA hydrogel composition used: 20% AAc, 8.8% APS.

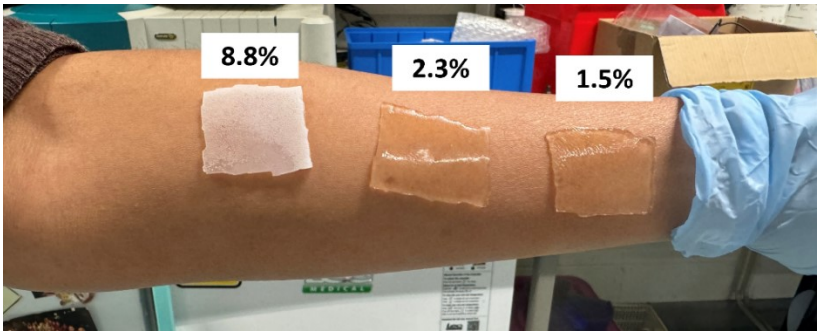

Figure S6. Photographs of hydrogel films on a participant arm with varying APS concentrations. PAAc-co-MBA hydrogel composition used: 20% AAc, 0.15% MBA. As the oxidant concentration increases, that leads to the aggregation of polymer, and the hydrogel exhibits a milky and translucent appearance.

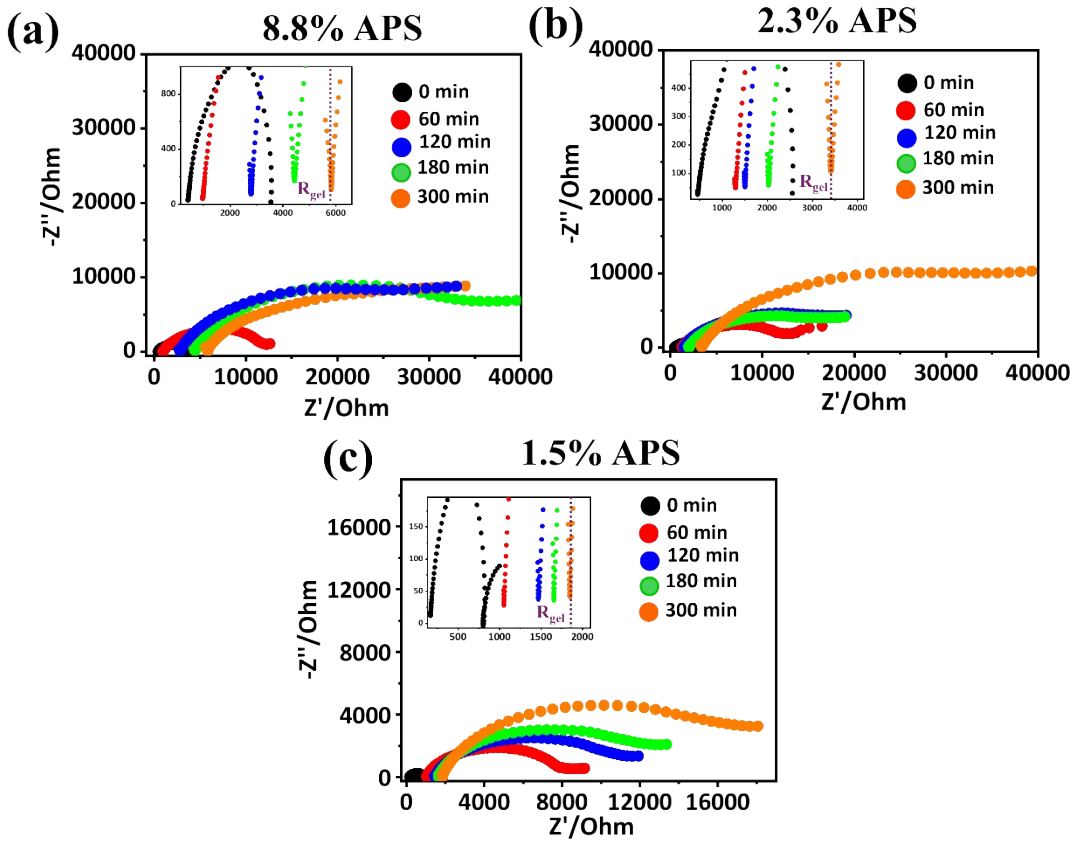

Figure S7. Nyquist plots collected at various swelling time points (0-300 min). PAAc-co-MBA hydrogel composition: 20% AAc, 0.15% MBA) (n=3) with varying APS concentrations. The high-frequency intercept of the semi-circle on the real impedance axis (Z'), marked as R_{gel}, corresponds to the bulk hydrogel resistance and is used throughout this work as the key impedance-derived quantitative measure of hydrogel swelling.

These data confirm that the characteristic high-frequency semi-circle associated with the bulk hydrogel response and the lower-frequency interfacial component are retained across all oxidant concentrations, while the magnitude of R_{gel} varies systematically with formulation. Overall, these results demonstrate that R_{gel} is a robust and sensitive parameter for monitoring formulation-dependent hydrogel swelling behaviour.

pK_a values of PAAc-co-MBA hydrogels were determined by fitting a logistic sigmoidal growth model (Equation S1) to experimental data presented in Section 3.1:

$$y = \frac{a}{(1 + exp(-k \times (x - x_c)))} \quad \text{(S1)}$$

where, k is the rate constant, x represents the pH of the solution, x_c is the inflection point of the sigmoidal curve that represents pK_a, and a is the asymptote.

Table S4. $\Delta\%R_{gel}$ and $\Delta\%G_{gel}$ values of PAAc-co-MBA hydrogels as a function of solute pH. (IS 0.01) by a logistic sigmoidal growth model.

Parameter	a	x_c	k	χ^2	R^2
$\Delta\%R_{gel}$	590.12	4.1	0.87	34.81	0.97
$\Delta\%G_{gel}$	1864.35	5.29	1.42	19.12	0.99

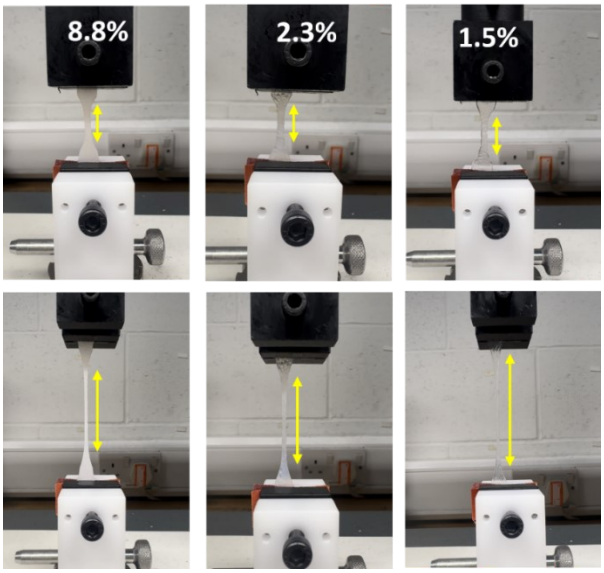

Figure S8. Photographs during tensile measurement of hydrogels with varying APS concentrations (as described in section 3.2). PAAc-co-MBA hydrogel composition used: 20% AAc, 0.15% MBA.

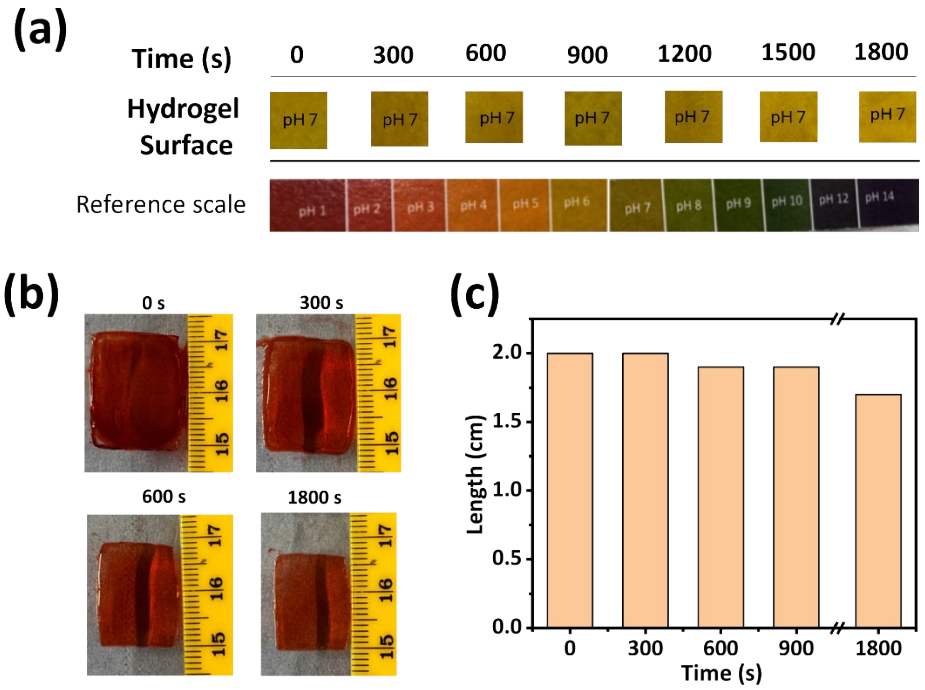

Figure S9. (a) pH indicator strip images showing control condition hydrogel maintained a constant neutral pH (pH 7) over 1800 s, and (b) Time-lapse images of hydrogel length (cm) at various time points (0-1800 s), showing no significant change in length within the first 600 s.

References:

1. Z. Hu, W. Tang and X. Ji, *Macromolecular Rapid Communications*, 2024, **45**, 2400371.
2. B. C. Smith, 2018.
3. S. W. Bae, J. S. Lee, V. M. Harms and W. L. Murphy, *Macromolecular bioscience*, 2019, **19**, 1800353.
4. R. Singh, D. Pal, A. Mathur, A. Singh, M. A. Krishnan and S. Chattopadhyay, *Reactive and Functional Polymers*, 2019, **144**, 104346.
5. K. A. Milakin, S. Gupta, L. Kobera, A. Mahun, M. Konefał, O. Kockova, O. Taboubi, Z. Morávková, J. M. Chin and K. Allahyarli, *ACS applied materials & interfaces*, 2023, **15**, 23813–23823.
6. B. Gieroba, G. Kalisz, M. Krysa, M. Khalavka and A. Przekora, *International journal of molecular sciences*, 2023, **24**, 2630.
7. Y. Li, Y. Ma, X. Jiao, T. Li, Z. Lv, C. J. Yang, X. Zhang and Y. Wen, *Nature Communications*, 2019, **10**, 1036.
8. L. Yang, B. Bai, C. Ding, H. Wang and Y. Suo, *RSC Advances*, 2016, **6**, 9507–9517.
9. A. Mignon, J. Vermeulen, G.-J. Graulus, J. Martins, P. Dubruel, N. De Belie and S. Van Vlierberghe, *Carbohydrate polymers*, 2017, **168**, 44–51.
10. M. Irfan, J. Zhai, Q. Li, S. Chen, G. X. Li and J. J. Xiao, *Journal of Polymer Science*, 2025, **63**, 342–357.